Squark Production at the Fermilab Tevatron

W. Beenakker, R. Höpker, M. Spira, and P. M. Zerwas
Deutsches Elektronen–Synchrotron DESY, D-22603 Hamburg, Federal Republic of Germany
(Received 9 December 1995)

We have determined the next-to-leading order QCD corrections to the production of squark-antisquark pairs in $p\bar{p}$ collisions. The renormalization scale dependence is reduced considerably. The production cross section at the Fermilab Tevatron increases by about a factor of 2 if we compare the next-to-leading order prediction at a scale near the squark mass with the lowest order for which, in the experimental analyses, the scale was identified with the invariant energy of the parton subprocesses. This results in a rise of the experimental lower bound on the squark mass from the Fermilab Tevatron by about 20 GeV.

PACS numbers: 14.80.Ly, 12.38.Bx, 13.85.Rm

The search for Higgs bosons and supersymmetric particles rank, *sub specie aeternitatis*, is among the most important experimental endeavors of high energy physics [1]. Both areas are closely related through the hierarchy problem. In fact, the idea of a supersymmetric extension of the standard model is qualitatively supported, though not proved, by the successful prediction of the electroweak mixing angle. The colored particles, i.e., squarks and gluinos, of supersymmetric theories can be searched for most efficiently at the Fermilab Tevatron $p\bar{p}$ collider and, in the future, at the CERN Large Hadron Collider up to very high mass values. Lower bounds on the squark and gluino masses have been set by both the Fermilab Tevatron experiments CDF and D0. At the 90% C.L., the masses are larger than about 148 GeV for gluino masses below 400 GeV [2,3].

The evaluation of the experimental data has been based so far on the lowest-order (LO) production cross sections [4–7], Figs. 1(a) and 1(e). In order to improve the theoretical predictions for the $p\bar{p}$ cross sections, the QCD corrections have to be evaluated in next-to-leading order (NLO). The theoretical analysis is straightforward but very tedious due to the large variety of production channels and final states. We report in this Letter, as a first indispensable step, on the production of squark-antisquark pairs:

$$p\bar{p} \to \tilde{q}\bar{\tilde{q}} + X \quad \text{for } \tilde{q} \neq \tilde{t}\,. \tag{1}$$

The $\tilde{q}_L/\tilde{q}_R$ splitting, particularly important for stop particles as well as the analysis of gluino final states [8], will be discussed in a more comprehensive report at a later time. For the sake of simplicity we have taken all squark states mass degenerate, i.e., the $n_{\tilde{q}} = 5$ squark states in the final state as well as the stop particles, which appear in internal loops. The only free parameters are therefore the masses of the squarks and gluinos, $m_{\tilde{q}}$ and $m_{\tilde{g}}$, respectively. The top mass is fixed to $m_t = 174$ GeV [10].

The next-to-leading order QCD calculation has been performed in the Feynman gauge, and the singularities have been isolated by means of dimensional regularization. The masses have been renormalized in the on-shell scheme. The massive particles are decoupled smoothly for momenta smaller than their masses within the modified $\overline{\text{MS}}$ (minimal subtraction) scheme [11]. When removing the infrared divergences, a cutoff Δ was introduced for the invariant mass of the squark-gluon system in the final state, which separates soft from hard gluon radiation [9]. If both contributions are added, any Δ dependence disappears from the total cross section for $\Delta \to 0$. The remaining collinear mass singularities can be absorbed into the renormalization of the parton densities [12] carried out in the $\overline{\text{MS}}$ factorization scheme. The Glück-Reya-Vogt (GRV) parametrizations of the parton densities [13] have been adopted, which allow for proper LO and NLO comparisons; CTEQ2 [14] and MRSH [15] parametrizations have also been used for assessing the uncertainties from the parton densities.

If the squarks are lighter than the gluinos, squarks can also be decay products of on-shell gluinos, $\tilde{g} \to \tilde{q}\bar{q}$, etc. Since we focus in the present analysis on the evaluation of the QCD corrections, we shall restrict ourselves to irreducible final states in which squarks do not evolve from on-shell gluinos; after gluino final states are included explicitly, this technical assumption will dissolve *eo ipso*. For the wedge $m_{\tilde{q}} > m_{\tilde{g}}$ we disregard, in the same sense as above, the decay of the squarks to gluinos.

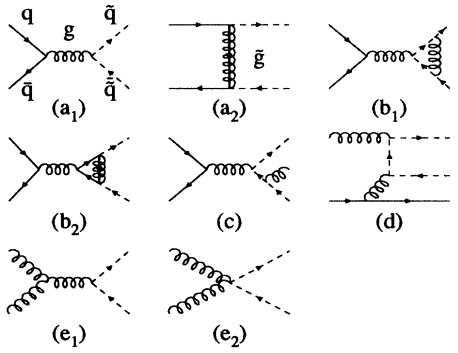

FIG. 1. Generic diagrams for squark-antisquark pair production: (a_1), (a_2) basic Born-level $q\bar{q}$ diagrams; (b_1), (b_2) vertex corrections due to gluon and gluino exchange; (c) gluon emission; (d) gluon-quark process; (e_1), (e_2) gluon fusion.

 © 1995 The American Physical Society

Since quark-quark pair initial states give negligible contributions to the generation of high invariant mass states in $p\bar{p}$ collisions, the cross section is built up primarily by quark-antiquark annihilation and, to a lesser extent, by gluon fusion.

Quark-antiquark initial states.—The subprocesses $q\bar{q} \to \tilde{q}\bar{\tilde{q}}$ are described to leading order, Figs. 1(a_1) and 1(a_2), by mixtures of amplitudes appropriate to unlike/like flavors and helicities. Typical standard QCD and supersymmetric vertex corrections are displayed in Figs. 1(b_1) and 1(b_2). Ordinary gluon radiation and a diagram related to the renormalization of the parton densities are exemplified in Figs. 1(c) and 1(d). Note that $\tilde{q}\bar{\tilde{q}}$ pairs can be generated in qg collisions only in next-to-leading order.

The diagrams have been evaluated analytically to obtain the double differential cross sections $d\hat{\sigma}_{ij}/d\hat{t}\,d\hat{u}$ at the parton level; i, j are the parton indices $g, q, \bar{q}$ and $\hat{t}, \hat{u}$ are the usual Mandelstam momentum transfer variables. The total cross sections $\hat{\sigma}_{ij}$ may be expressed in terms of scaling functions f_{ij},

$$\hat{\sigma}_{ij} = \frac{\alpha_s^2(Q^2)}{m_{\tilde{q}}^2}\left\{ f_{ij}^{(0)}(\eta; r) + 4\pi\alpha_s(Q^2)\left[f_{ij}^{(1)}(\eta; r, r_t) + \bar{f}_{ij}^{(1)}(\eta; r)\ln\left(\frac{Q^2}{m_{\tilde{q}}^2}\right)\right]\right\}. \tag{2}$$

They depend on the invariant parton energy $\sqrt{\hat{s}}$ through $\eta = \hat{s}/4m_{\tilde{q}}^2 - 1$, and on the ratios of the particle masses $r = m_{\tilde{g}}/m_{\tilde{q}}$, $r_t = m_t/m_{\tilde{q}}$. α_s is the QCD coupling constant. Renormalization and factorization scales are identified for the sake of simplicity, $\mu_R = \mu_F = Q$. $f_{ij}^{(0)}$ denotes the lowest-order contributions. While $f_{qg}^{(0)}$, the scaling function associated with qg collisions, is zero for $\tilde{q}\bar{\tilde{q}}$ production, a compact expression [5] can be found for quark-antiquark initial states,

$$f_{q\bar{q}}^{(0)}(\eta; r) = \frac{\pi\beta}{108(1+\eta)}\left\{\left[\frac{1+r^2}{\beta(1+\eta)} + 2\beta\right]6L_r - 24 + \frac{48r^2(1+\eta)}{(1+r^2)^2 + 4\beta^2 r^2(1+\eta)} + 4n_{\tilde{q}}\beta^2 + 2\beta\left[-\frac{L_r}{1+\eta}\left(r^2 + \frac{(1+r^2)^2}{4\beta^2(1+\eta)}\right) + 2\beta + \frac{1+r^2}{\beta(1+\eta)}\right]\right\}, \tag{3}$$

$$f_{q'\bar{q}}^{(0)}(\eta; r) = \frac{\pi\beta}{108(1+\eta)}\left\{\left[\frac{1+r^2}{\beta(1+\eta)} + 2\beta\right]6L_r - 24 + \frac{48r^2(1+\eta)}{(1+r^2)^2 + 4\beta^2 r^2(1+\eta)}\right\}, \tag{4}$$

where $L_r = \ln(x_+/x_-)$ with $x_\pm = 1 + r^2 \pm 2\beta/(1 \mp \beta)$ and $\beta = (1 - 4m_{\tilde{q}}^2/\hat{s})^{1/2}$. The scaling functions $f_{ij}^{(1)}$ and $\bar{f}_{ij}^{(1)}$, describing the next-to-leading order corrections, are displayed in Fig. 2. The scaling functions $f_{ij}^{(1)}$ are split into the "virtual + soft" part ($V + S$) and the "hard" part (H) into which the infrared $\ln^j\Delta$ ($j = 1, 2$) singularities of the ($V + S$) contribution are absorbed so that these functions are insensitive to the choice of $\Delta \to 0$. Near threshold, which is the kinematically most important region in $p\bar{p}$ collisions, the Sommerfeld rescattering contribution, due to the exchange of Coulomb gluons between the slowly moving $\tilde{q}\bar{\tilde{q}}$ pairs, leads to a singularity $\sim \pi\alpha_s/\beta$ which neutralizes the phase space suppression near threshold,

$$f_{q\bar{q}}^{(1)\mathrm{thr}}(\eta; r) = f_{q\bar{q}}^{(0)\mathrm{thr}}(\eta; r)\left\{\frac{7}{48\beta} + \frac{2}{3\pi^2}\ln^2(8\beta^2) - \frac{11}{4\pi^2}\ln(8\beta^2)\right\} \quad \text{with } f_{q\bar{q}}^{(0)\mathrm{thr}}(\eta; r) = \frac{4\pi\beta r^2}{9(1+r^2)^2}. \tag{5}$$

The same relations hold for unlike flavors near threshold. The $\ln^2\beta$ terms, generated by initial state gluon radiation near threshold, can be exponentiated [16]. The plateaus for large parton energies are due to flavor-excitation and gluon-splitting mechanisms [cf. Fig. 1(d)]. The t- and u-channel exchanges of gluons lead to an asymptotically constant cross section, the scale of which is set by the squark mass, i.e., $\hat{\sigma} \sim \alpha_s^3/m_{\tilde{q}}^2$, to be contrasted with the scaling behavior $\hat{\sigma} \sim \alpha_s^2/s$ of the cross section to lowest order. The values of the scaling functions in the asymptotic plateau region can be calculated analytically, $f_{qg,H}^{(1)} \to 2159/19\,440\pi$ and $\bar{f}_{qg}^{(1)} \to -11/324\pi$.

Gluon-gluon initial states.—To lowest order the diagrams contributing to the subprocess $gg \to \tilde{q}\bar{\tilde{q}}$ are the well-known diagrams from quark-pair production [e.g., Fig. 1(e_1)] supplemented by the seagull term Fig. 1(e_2) for scalar squarks. Carrying out the next-to-leading order program, we find, in the same notation as above [5],

$$f_{gg}^{(0)}(\eta; r) = \frac{n_{\tilde{q}}\pi\beta}{96(1+\eta)^2}\left\{\frac{41}{2} + 5\eta + \left(\frac{8}{\beta} + \frac{1}{2\beta(1+\eta)}\right)\ln\left(\frac{1-\beta}{1+\beta}\right)\right\}. \tag{6}$$

The gg scaling functions are displayed in Fig. 2(d) in leading and next-to-leading order. Near the threshold, the

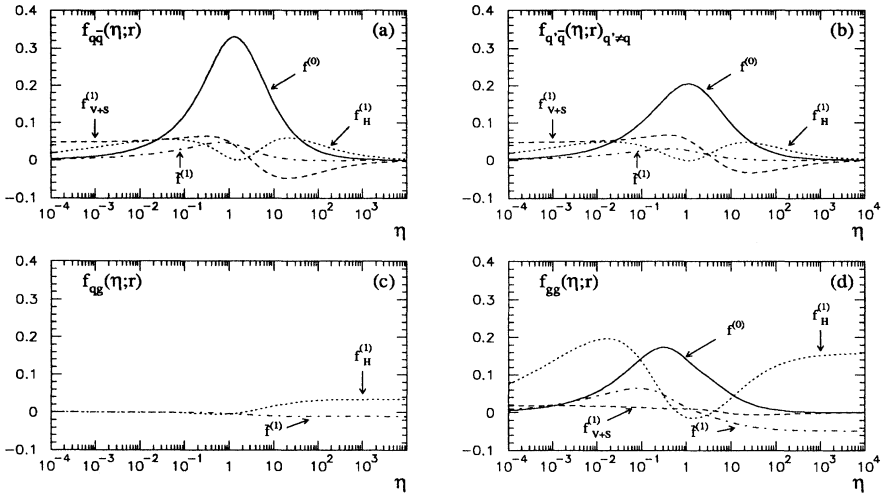

FIG. 2. The scaling functions for squark-antisquark pair production in (a) $q\bar{q}$, (b) $q'\bar{q}$, (c) qg, and (d) gg collisions. The notation follows Eq. (2) with $\eta = \hat{s}/4m_{\tilde{q}}^2 - 1$; $V + S$ denotes the sum of the virtual and soft corrections, H the contribution of hard gluon emission. Mass parameters $m_{\tilde{q}} = 250$ GeV and $m_{\tilde{g}} = 200$ GeV.

Sommerfeld enhancement is observed again in next-to-leading order,

$$f_{gg}^{(1)\mathrm{thr}}(\eta) = f_{gg}^{(0)\mathrm{thr}}(\eta)\left\{\frac{11}{336\beta} + \frac{3}{2\pi^2}\ln^2(8\beta^2) - \frac{183}{28\pi^2}\ln(8\beta^2)\right\} \quad \text{with } f_{gg}^{(0)\mathrm{thr}}(\eta) = \frac{7n_{\tilde{q}}\pi\beta}{192}. \tag{7}$$

The high-energy plateaus are generated as before by flavor-excitation and gluon-splitting mechanisms, $f_{gg,H}^{(1)} \to 2159/4320\pi$ and $\bar{f}_{gg}^{(1)} \to -11/72\pi$.

While for $\alpha_s \sim 0.1$ the higher-order corrections are suppressed significantly with respect to the Born term for quark initial states, the large color charge of gluons leads to corrections of the order of the Born term for the gg initiated subprocess.

(i) It is obvious from Fig. 3(a) that the theoretical predictions for the $p\bar{p} \to \tilde{q}\bar{\tilde{q}}$ production process are improved considerably by taking into account the next-to-leading order QCD corrections. While the dependence on the renormalization/factorization scale Q is quite steep and monotonic in leading order, the Q dependence is significantly reduced in next-to-leading order for reasonable variations of the scale, running even through a broad maximum near $Q \sim m_{\tilde{q}}/3$. Since the cross section is built up mainly by the quark channels ($\gtrsim 85\%$) and thus based on well-measured parton densities, the variation between different parton parametrizations is negligibly small.

TABLE I. K factors for a set of $\tilde{q}, \tilde{g}$ masses and a range of renormalization/factorization scales Q at the Fermilab Tevatron energy $\sqrt{s} = 1.8$ TeV; GRV parton densities [13].

$m_{\tilde{q}}$ (GeV)	$m_{\tilde{g}}$ (GeV)	$Q = m_{\tilde{q}}/3$	$Q = m_{\tilde{q}}$	$Q = 2m_{\tilde{q}}$
150	200	0.75	1.15	1.37
150	400	0.70	1.11	1.34
200	200	0.74	1.14	1.36
200	400	0.72	1.12	1.34
250	200	0.76	1.15	1.38
250	400	0.75	1.15	1.37
400	200	0.81	1.18	1.39
400	400	0.78	1.15	1.37

(ii) The K factors, defined as the ratio $K = \sigma_{\mathrm{NLO}}/\sigma_{\mathrm{LO}}$ (with all quantities in the numerator and denominator calculated consistently in NLO and LO, respectively), depend only mildly on the squark and gluino masses. Experimental mass bounds can therefore be corrected easily for higher-order QCD effects. A sample of K factors is collected in Table I for various choices of the renormalization/factorization scale parameter Q.

(iii) Finally in Fig. 3(b) we illustrate the impact of the QCD corrections on the experimental lower bounds of the squark masses. We compare the lowest-order cross section at $Q = \sqrt{\hat{s}}$, the scale adopted in experimental analyses, with the next-to-leading order prediction at $Q = m_{\tilde{q}}$ [17]. The NLO cross section is significantly larger at this theoretically reasonable scale than the LO cross section at the scale $\sqrt{\hat{s}}$. Taken at face value, this increases the bound on the squark mass by about 20 GeV. While no precise value of Q can be defined *a priori*, it is clear nevertheless that the experimental bounds derived from Fermilab Tevatron data [2,3] are *very* conservative and that the true bounds are likely to be higher by as much as ~20 GeV.

After these introductory remarks we present our final results in Fig. 3 and Table I. The cross sections of the various subprocesses have been convoluted with the parton densities in the GRV [13], CTEQ2 [14], and MRSH [15] parametrizations. The following conclusions can be drawn from the analysis of the figures and the table.

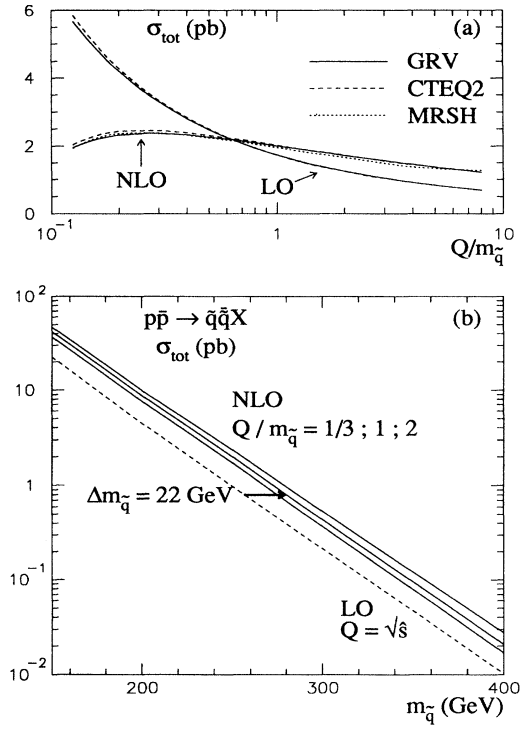

FIG. 3. Total cross section for the irreducible production of squark-antisquark pairs $p\bar{p} \to \tilde{q}\bar{\tilde{q}}X$ at the Fermilab Tevatron energy $\sqrt{s} = 1.8$ TeV. (a) Dependence on the renormalization/factorization scale Q for the leading order (LO) and the next-to-leading order (NLO) predictions, and sensitivity to different parton densities; mass parameters as in Fig. 2. (b) Dependence of the cross section on the squark mass for $m_{\tilde{g}} = 200$ GeV; GRV parton densities for NLO, and EHLQ parton densities for LO used in the experimental analysis [3]. Upper full line of the NLO prediction corresponds to the renormalization/factorization scale $Q/m_{\tilde{q}} = 1/3$, middle line $= 1$, and lower line $= 2$.

We thank S. Lammel for useful discussions on the Fermilab Tevatron squark and gluino mass limits and their theoretical basis.

[1] H. P. Nilles, Phys. Rep. **110**, 1 (1984); H. E. Haber and G. L. Kane, *ibid.* **117**, 75 (1985).

[2] CDF Collaboration, F. Abe *et al.,* Phys. Rev. Lett. **69**, 3439 (1992).

[3] S. Hagopian, in Proceedings of the XXVII International Conference on High Energy Physics, Glasgow, 1994 (to be published); Fermilab Report No. FERMILAB Conf 94/ 331-E, 1994; D. R. Claes, Fermilab Report No. FERMILAB Conf 94/ 290-E, 1994; S. Lammel, in Proceedings of the DESY Theory Workshop on Supersymmetry, Hamburg, 1994 (to be published).

[4] G. L. Kane and J. P. Leveille, Phys. Lett. B **112**, 227 (1982).

[5] P. R. Harrison and C. H. Llewellyn Smith, Nucl. Phys. **B213**, 223 (1983); **B223**, 542(E) (1983).

[6] E. Reya and D. P. Roy, Phys. Rev. D **32**, 645 (1985); H. Baer and X. Tata, Phys. Lett. B **160**, 159 (1985).

[7] H. Baer, F. E. Paige, S. D. Protopopescu, and X. Tata, Report on ISAJET 7.0/ ISASUSY 1.0, Report No. FSU-HEP 930329 and Report No. UH-511-764-93, 1993 (unpublished).

[8] The top-quark analog of the QCD corrections to gluino-pair production in gg fusion, with squark loops left out however, has been presented in Ref. [9].

[9] W. Beenakker, H. Kuijf, W. L. van Neerven, and J. Smith, Phys. Rev. D **40**, 54 (1989).

[10] CDF Collaboration, F. Abe *et al.*, Phys. Rev. Lett. **73**, 225 (1994); Phys. Rev. D **50**, 2966 (1994).

[11] J. Collins, F. Wilczek, and A. Zee, Phys. Rev. D **18**, 242 (1978); W. J. Marciano, *ibid.* **29**, 580 (1984); P. Nason, S. Dawson, and R. K. Ellis, Nucl. Phys. **B303**, 607 (1988).

[12] G. Altarelli, R. K. Ellis, and G. Martinelli, Nucl. Phys. **B157**, 461 (1979); W. Furmanski and R. Petronzio, Z. Phys. C **11**, 293 (1982).

[13] M. Glück, E. Reya, and A. Vogt, Z. Phys. C **53**, 127 (1992).

[14] CTEQ Collaboration, J. Botts *et al.,* Phys. Lett. B **304**, 159 (1993); CTEQ2 Collaboration, J. Botts *et al.,* Report No. MSUHEP-93/28, 1993.

[15] A. D. Martin, W. J. Stirling, and R. G. Roberts, in *Proceedings of the Workshop on Quantum Field Theoretical Aspects of High Energy Physics,* edited by B. Geyer and E.-M. Ilgenfritz (ZHS University, Leipzig, 1993).

[16] A. H. Mueller and P. Nason, Phys. Lett. B **156**, 226 (1985); Nucl. Phys. **B266**, 256 (1986).

[17] The scale $\sqrt{\hat{s}}$ cannot be used in NLO; see J. C. Collins, D. E. Soper, and G. Sterman, in *Perturbative Quantum Chromodynamics,* edited by A. H. Mueller (World Scientific, Singapore, 1989).